Magnetic Resonance in Medicine 41:469–473 (1999)

Simultaneous Recording of Evoked Potentials and T_2^*-Weighted MR Images During Somatosensory Stimulation of Rat

Gerrit Brinker, Christian Bock, Elmar Busch, Henning Krep, Konstantin-Alexander Hossmann, and Mathias Hoehn-Berlage

Somatosensory evoked potentials (SEP) and T_2^*-weighted nuclear magnetic resonance (NMR) images were recorded simultaneously during somatosensory stimulation of rat to investigate the relationship between electrical activation of the brain tissue and the signal intensity change in functional NMR imaging. Electrical forepaw stimulation was performed in Wistar rats anesthetized with α-chloralose. SEPs were recorded with calomel electrodes at stimulation frequencies of 1.5, 3, 4.5, and 6 Hz. At the same time, T_2^*-weighted imaging was performed, and the signal intensity increase during stimulation was correlated with the mean amplitude of the SEP. Both the stimulation-evoked signal intensity increase in T_2^*-weighted images and the amplitude of SEPs were dependent on the stimulation frequency, with the largest signals at a stimulation frequency of 1.5 Hz and decreasing activations with increasing frequencies. The feasibility of simultaneous, artifact-free recordings of T_2^*-weighted NMR images and of evoked potentials is proved. Furthermore, the study demonstrates—in the intact brain—the validity of functional magnetic resonance imaging for estimating the intensity of electrocortical activation. Magn Reson Med 41:469–473, 1999.

Key words: fMRI; somatosensory cortex; evoked potentials; electrophysiology; rat

In recent years nuclear magnetic resonance (NMR) imaging has gained widespread use in the investigation of functional brain activation in both humans and animal experiments (1–5). It is widely accepted that the increased energy demands of the activated brain tissue result in an increase in local cerebral blood flow (CBF), although the exact mechanisms of coupling between CBF and neuronal activation are still under discussion (6–11). The amount of CBF increase during somatosensory stimulation exceeds the increase in cerebral metabolic rate of oxygen ($CMRO_2$) (12,13), with the consequence that the net oxygen extraction fraction decreases. This results in decreased local concentration of deoxyhemoglobin, which is paramagnetic, and therefore in a change of the magnetic susceptibility of the blood. As a consequence, the signal intensity in T_2^*-weighted MR images increases, a mechanism that has been referred to as blood oxygenation level-dependent (BOLD) contrast (14,15). T_2^*-weighted MR imaging sequences are widely used for the mapping of cortical functions in humans (16,17) and more recently also in animals (18,19). The functional response to somatosensory stimulation has been shown by perfusion-weighted imaging with visualization of both the spatial distribution and the temporal pattern of the activation-induced changes in blood flow (20,21). However, it must be kept in mind that imaging of functional activation relies on the intact coupling with blood flow and metabolism and, therefore reflects neuronal activity only indirectly. For a more precise evaluation, functional MR imaging should therefore be compared with the electrophysiological response. The present investigation demonstrates for the first time the feasibility of simultaneous measurements of somatosensory evoked cortical potentials (SEPs) and T_2^*-weighted images in the rat.

MATERIALS AND METHODS

Animal Preparation

Five male Wistar rats (350–400 g BW) were anesthetized with 1.2% halothane in a 70%/30% mixture of N_2O/O_2. Body temperature was maintained at 37°C via a rectal thermometer and a feedback-controlled warm water blanket. Two PE 50 catheters were placed in the right femoral artery and femoral vein, to draw blood samples for arterial blood gas analysis and to infuse drugs, respectively. After tracheotomy the trachea was cannulated and the animals were artificially ventilated to keep pCO_2 in the physiological range. Pancuronium bromide (0.2 mg/kg/hr) was given for muscle relaxation.

After placing the animals prone in a Plexiglas stereotactic headholder, the skin and the periosteum over the skull were medially incised and retracted. A small nylon nut was glued to the exposed nasal bone and another one to the skull at the level of the somatosensory cortex (1 mm anterior to the bregma). The remaining skull surface was covered with dental cement to avoid NMR imaging artifacts caused by susceptibility changes. For electroencephalographic (EEG) recording inside the magnet, two L-shaped calomel electrodes were prepared as described before (22). The electrodes were introduced with their tip into each nut, with the active electrode at the level of the somatosensory cortex and the reference electrode above the nasal bone, and fixed at the stereotactic holder. With the setup described, electrophysiological recording inside the magnet is possible with minimal artifacts.

Sixty minutes before MR measurements, α-chloralose (80 mg/kg) was given intravenously and supplemented by 40 mg/kg i.v. at 90 min intervals. Halothane anesthesia was discontinued, and N_2O was substituted by N_2. A pair of needle electrodes was introduced into the skin of the left

Max-Planck-Institute for Neurological Research, Cologne, Germany.

Grant sponsor: Deutsche Forschungsgemeinschaft; Grant number: SFB 194/B1.

*Correspondence to: Dr. Mathias Hoehn-Berlage, In-vivo-NMR, Max-Planck-Institut für neurologische Forschung, Gleueler Str. 50, D-50931 Köln, Germany. E-mail: mathias@mpin-koeln.mpg.de.

Received 20 March 1998; revised 30 July 1998; accepted 10 August 1998.

forepaw. Rectangular electrical pulses of 0.3 msec duration and 0.5 mA intensity were applied at frequencies of 1.5, 3.0, 4.5, or 6.0 Hz for a duration of 50 sec. The pulses were delivered by a constant current power supply (FMI, Egelsbach, Germany). In addition to this protocol, in one experiment the left hindpaw was stimulated at 1.5 Hz with electrical pulses of 0.3 msec and 1.2 mA intensity.

NMR Methods

NMR measurements were performed on a 4.7 T Bruker BIOSPEC MSL-X11 system (Bruker, Ettlingen, Germany) equipped with actively shielded gradient coils (100 mT/m, rise time <250 μsec). Radiofrequency (RF) pulses were transmitted using a 12 cm diameter Helmholtz coil, while signals were received with a 16 mm diameter inductively coupled surface coil centered over the bregma. MR images were acquired using the fast low-angle shot (FLASH) sequence (23) with a field of view of 4 cm. Multislice pilot scans of the brain anatomy (flip angle α 22.5°, TE 8 msec, TR 400 msec) were performed to position the functional image slice. Single-slice heavily T_2^*-weighted images (24) ($\alpha = 22.5°$, TE 60 msec, TR 70 msec, slice thickness 2 mm, 64 phase encoding steps, scan time 4.5 sec) were recorded for functional imaging.

Experimental Protocol

Based on the sagittal pilot scans, the functional imaging slice was positioned coronally through the somatosensory cortex 1.0 mm anterior to the bregma. Each set of activation experiments included the acquisition of eight T_2^*-weighted images (T_2^*-WI) prior to stimulation (baseline images) and eight images during electrical stimulation of paws. This procedure was repeated in each animal for the various stimulation frequencies, with a rest period of at least 5 min between each stimulation sequence. To avoid misinterpretations due to habituation effects, the order of stimulation frequencies was varied. EEG recording artifacts due to desiccation of the electrodes were prevented by refilling the saline solution in the nylon nuts several times during the course of the experiment.

Data Processing

T_2^*-WI activation maps were obtained by subtracting the eight averaged baseline images from the eight averaged stimulation images of each stimulation sequence. For localization of the functionally activated brain region, pixels with an intensity of more than 1.5 standard deviations above the noise level of subtracted images were overlaid onto the corresponding anatomical picture. Quantitative analysis of functional (f)MRI was performed by measuring the T_2^*-WI signal intensity increase in a region of interest placed in the center of the activated somatosensory cortex.

EEGs and evoked electrical responses were recorded using a laboratory computer. Forepaws were stimulated at increasing frequencies (1.5, 3, 4.5, and 6 Hz, respectively), and the cortical evoked potentials were averaged over the total stimulation period of 50 sec, resulting in averages of 75, 150, 225, and 300 single responses, respectively. The frequency dependent changes of the peak-to-peak amplitude (difference between P1- and N1-signals) were expressed in percent of the mean amplitude at 1.5 Hz.

Statistical analysis (Student's *t*-test, unpaired, unequal variances) was performed by comparison of the normalized peak-to-peak SEP amplitude and the T_2^*-WI signal intensity increase, respectively, obtained at 1.5 Hz with the corresponding values at higher stimulation frequencies.

RESULTS

Physiological variables were kept within normal range during the whole length of experiments: arterial PO_2 was 135 ± 26 mmHg, arterial CO_2 was 37.5 ± 4.2 mmHg, arterial pH was 7.37 ± 0.05, and the mean arterial blood pressure was 105 ± 9 mmHg (all values are means $\pm$ SD). During electrical stimulation physiological variables, notably systemic arterial pressure, did not change.

The novel experimental setup allowed simultaneous, artifact-free measurements of SEP and T_2^*-WI (Fig. 1). Artifacts in MR images, when present, were due to inhomogeneities of susceptibility produced by small air bubbles in the dental cement or the nylon nuts, or they appeared when the electrodes were placed on the skull with too high pressure. They could be eliminated by exchange of cement or revision of electrode placement. Gross disturbances of the electrical signal were visible during gradient switching but disappeared almost completely on averaging.

The SEPs consisted of an early negative deflection (N1-wave) with a peak latency between 14 and 18 msec, followed by a later positive deflection (P1-wave) with a latency of about 40 ms (Fig. 1, right column). N2-waves were detectable in some cases. The amplitude of the SEP was clearly dependent on stimulation frequency, with the largest amplitude at a stimulation frequency of 1.5 Hz and decreasing amplitudes with increasing frequency.

Electrical stimulation of the left forepaw resulted in an increase in T_2^*-WI signal intensity in the right somatosensory cortex (Fig. 1, left column). The signal intensity increase, expressed in percent of the resting level, was also dependent on the stimulation frequency, with the highest increase at 1.5 Hz ($5.91 \pm 0.83\%$, mean $\pm$ SEM) and decreasing signal intensity increases with increasing frequency ($3.42 \pm 0.58\%$ at 3 Hz, $1.56 \pm 0.56\%$ at 4.5 Hz, and $1.19 \pm 0.22\%$ at 6 Hz). Similarly, the peak-to-peak amplitude of the SEP was largest at 1.5 Hz and gradually declined with increasing frequencies (Fig. 1).

In one experiment a T_2^*-WI signal intensity increase was documented during stimulation of the left hindpaw, but the current required for activation was higher (0.3 msec, 1.2 mA). The cortical area activated by hindpaw stimulation was located in a slice 1.5 mm caudally from that of the forepaw, i.e., the area corresponding to the anatomical representation of the hindpaw in the rat cerebral somatosensory cortex (25) (Fig. 2).

In individual experiments, the correlation between SEP amplitude and T_2^*-WI signal intensity change at varying stimulation frequencies resulted in correlation coefficients ranging between 0.61 and 0.85 (example of one animal given in Fig. 3). For overall characterization of the frequency dependence of SEP and T_2^*-WI, the SEP amplitudes of individual animals were normalized to the mean amplitude at a stimulation rate of 1.5 Hz. The two variables

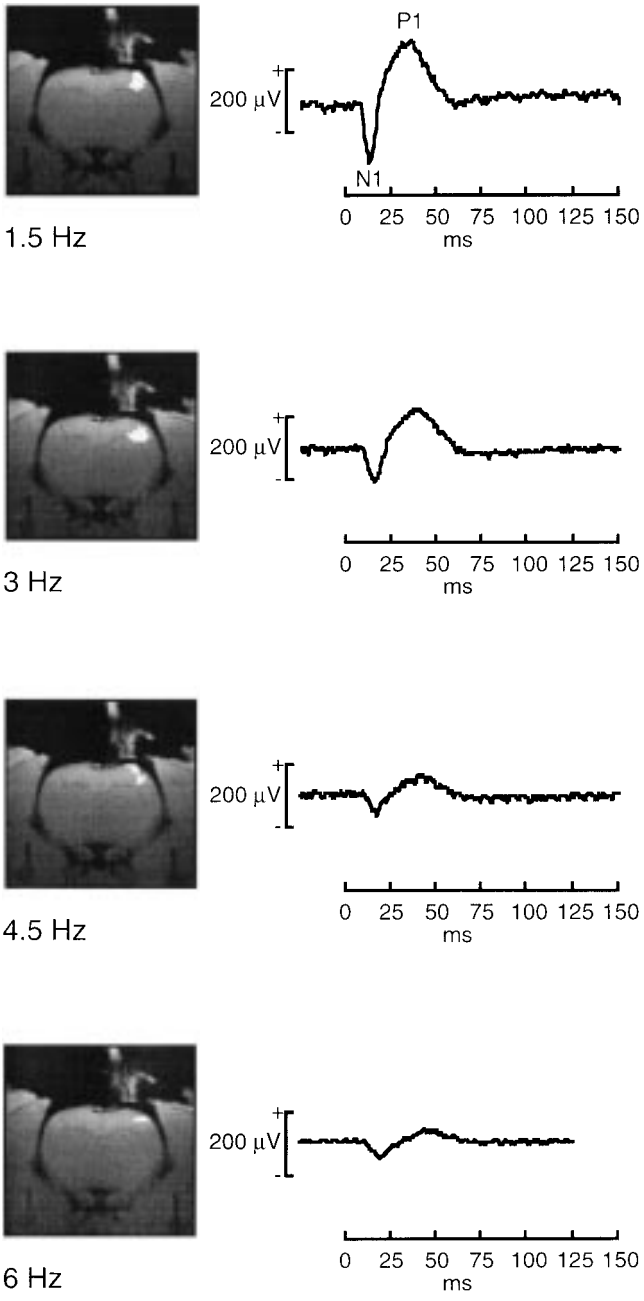

FIG. 1. Simultaneous acquisition of activation maps (left) and of somatosensory evoked potentials (right) at increasing stimulation frequencies (1.5, 3, 4.5, and 6 Hz) during left forepaw stimulation. Activation maps were derived from T2*-weighted images and overlaid on the corresponding anatomical image. The signal intensity increase is highest at 1.5 Hz (5.9 ± 0.8% above background, mean ± SEM) and decreases at increasing frequencies. Similarly, the amplitude of the SEP is largest at 1.5 Hz and gradually decreases at increasing frequencies. Note the position of the active electrode in the same image plane as that of the activated cortical field.

revealed a clearly similar behavior, namely, decreasing signals with increasing stimulation frequencies (Fig. 4: 5.91 ± 0.83% at 1.5 Hz, 3.42 ± 0.58% at 3 Hz, 1.56 ± 0.56% at 4.5 Hz, and 1.19 ± 0.22% at 6 Hz for BOLD signal intensity increase; 100 ± 7% at 1.5 Hz, 52 ± 2% at 3 Hz, 34 ± 5% at 4.5 Hz, and 22 ± 2% at 6 Hz for normalized SEP amplitude; all values mean ± SEM). The values recorded at 1.5 Hz differed significantly from the higher stimulation frequencies, both for the electrophysiological and for the MR data.

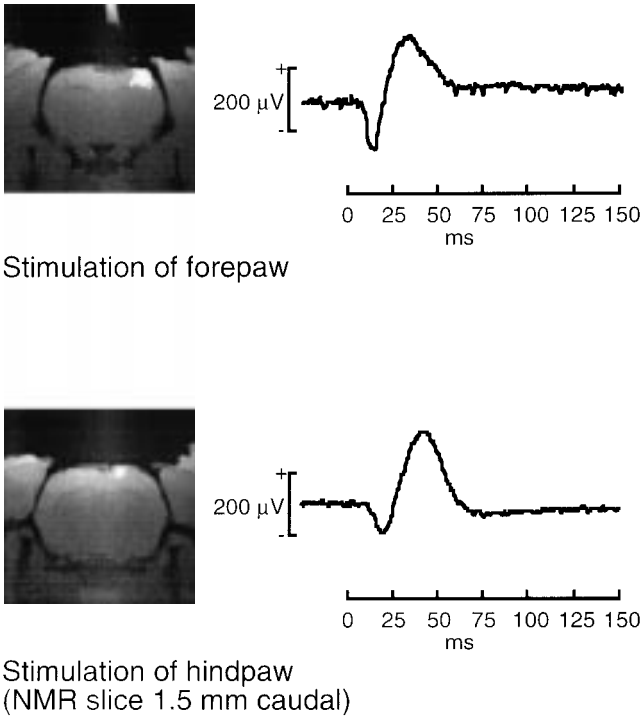

FIG. 2. Activation maps (left) and corresponding somatosensory evoked potentials (right) during stimulation at 1.5 Hz of left forepaw (top) and hindpaw (bottom). The planes in which cortical activity are visible are separated by 1.5 mm. Note the increased latency of the SEP and the medio-caudal shift of the activated cortical region during hindpaw stimulation as apparent by the relative shift of the epicenter of the activated regions for the representation of the forepaw and hindpaw in the somatosensory cortex (34).

DISCUSSION

The amplitude of evoked cortical potential depends, in the first place, on the intensity of the afferent cortical input. At

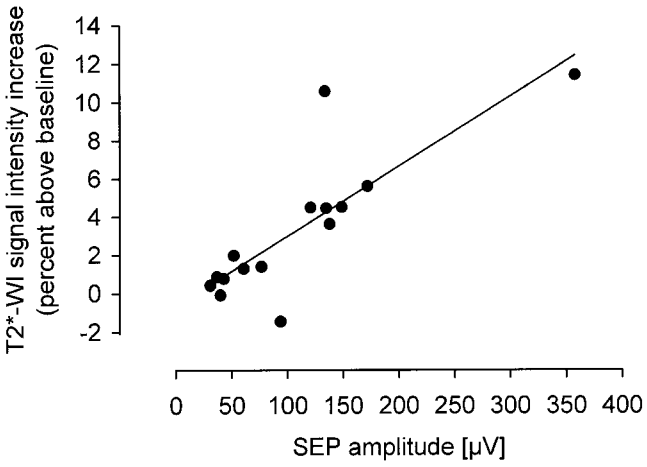

FIG. 3. Correlation of the increase of T2*-weighted imaging signal intensity with the peak-to-peak amplitude of the somatosensory evoked potential (SEP) during forepaw stimulation at increasing frequencies (data are from one individual animal; r = 0.82).

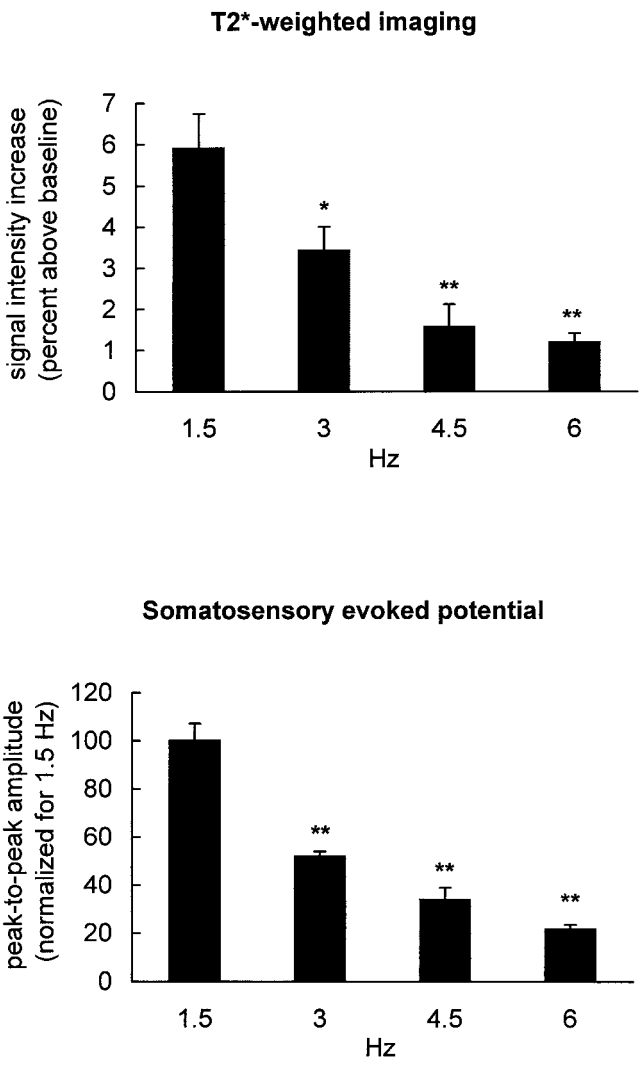

FIG. 4. Increase of signal intensity in T_2^*-weighted images (top) and normalized SEP amplitudes (bottom) at increasing stimulation frequencies. SEP amplitudes were normalized to the 1.5 Hz value. Note the similar frequency dependence of MR and SEP (mean ± SEM, statistically significant difference from 1.5 Hz: *, $P < 0.05$, **, $P < 0.01$).

a given stimulation intensity, it also reflects the level of oxygen consumption, at least under conditions of decreased metabolic rate. In dogs that underwent hypoxia and reoxygenation, the peak-to-peak amplitude of the SEP correlated with $CMRO_2$, irrespective of blood flow changes (26), and in humans metabolic and electrophysiological changes paralleled each other during controlled hypotension (27). On the other hand, activation of the neuronal network, which underlies the generation of evoked potentials, results in a coupled increase of glucose and—to a lesser degree—oxygen consumption, which rises with the intensity of the stimulation. It is therefore reasonable to assume that the amplitude of evoked potentials is a marker of the metabolic rate in the area in which the potentials are generated.

Changes in metabolic activity are also reflected by changes in T_2^*-WI signal intensity. A mathematical model of the relationship between $CMRO_2$, blood flow and T_2^*-WI signal intensity increase was recently presented by Buxton and Frank (15). According to their analysis, the increase of blood flow during stimulation is tightly coupled to the metabolic demand, although in a nonlinear relationship. Thus a small increase in metabolism requires a large increase in blood flow to compensate for the higher energy demands. In their proposed model, the relation between blood flow and MR signal intensity increase is nearly linear. Therefore, differences in the metabolic demand during different stimulation paradigms should have their counterparts in parallel changes of the corresponding MR signal intensity. This is supported by a recent NMR spectroscopy study that demonstrated parallel changes in T_2^*-WI signal and oxidative glucose metabolism during functional activation in rat (28).

The dependence of T_2^*-WI signal intensity on the frequency of somatosensory stimulation was first described by Gyngell et al in a model similar to that in the present study (24). Although in our study the T_2^*-WI signal elevations were somewhat smaller, the dependence of the MR signal on the stimulation frequency was similar, with the highest signal increase at 1.5 Hz and a gradual decline of signals at increasing frequencies (24). The most likely explanation for the frequency-dependent signal decline is the occlusion of the electrophysiological response at higher stimulation rates. In fact, in an earlier study of forepaw stimulation in cat, each stimulus evoked a maximal electrocortical response at low frequencies (2–3 Hz), whereas at higher frequencies every second or third evoked response was suppressed, resulting in a smaller averaged SEP amplitude (29). These authors also showed that the increase in microflow declined with increasing stimulation frequencies, which is in line with the interpretation that the hemodynamic-metabolic response is coupled to the metabolic demands of the activated tissue. The SEP amplitude, therefore, reflects the local cortical metabolic activation, which in turn can be detected by recording either microflow or T_2^*-WI signal intensity.

Obviously, the changes in T_2^*-WI during functional activation rely on the intact coupling among electrical activation, oxygen consumption, and blood flow. In pathological situations such as after global ischemia (30), this is not always the case. After prolonged global forebrain ischemia, produced by the four-vessel occlusion model in rat, recovery of electrical activity was much faster than that of the hemodynamic-metabolic response (31). On the other hand, resuscitation after 10 min cardiac arrest in rats led to the parallel normalization of SEP and blood flow increase during electrical forepaw activation (32,33). The application of T_2^*-WI for evaluation of post-ischemic recovery may therefore lead to different results, depending on the preservation of the coupling mechanisms. To avoid misinterpretations, the simultaneous recording of the electrophysiological response is, therefore, recommended.

CONCLUSIONS

Our study demonstrates the feasibility of simultaneous electrophysiological and functional MRI measurements and provides a new approach for studying the relationship between electrophysiological activity and MR-visible changes in blood flow and blood oxygenation. In the healthy brain, the T_2^*-WI signal intensity increases linearly

with the SEP amplitudes, but this relationship may be lost under pathological conditions. The simultaneous recording of SEPs together with functional MRI facilitates the interpretation of such conditions and provides evidence on the hemodynamic-metabolic coupling of functional activity.

REFERENCES

1. Ashe J, Ugurbil K. Functional imaging of the motor system. Curr Opin Neurobiol 1994;4:832–839.
2. Hyder F, Behar KL, Martin MA, Blamire AM, Shulman RG. Dynamic magnetic resonance imaging of the rat brain during forepaw stimulation. J Cereb Blood Flow Metab 1994;14:649–655.
3. Le Bihan D, Jezzard P, Haxby J, Sadato N, Rueckert L, Mattay V. Functional magnetic resonance imaging of the brain. Ann Intern Med 1995;122:296–303.
4. Kleinschmidt A, Lee BB, Requardt M, Frahm J. Functional mapping of color processing by magnetic resonance imaging of responses to selective P- and M-pathway stimulation. Exp Brain Res 1996;110:279–288.
5. Scanley BE, Kennan RP, Cannan S, Skudlarski P, Innis RB, Gore JC. Functional magnetic resonance imaging of median nerve stimulation in rats at 2.0 T. Magn Reson Med 1997;37:969–972.
6. Sokoloff L. Relationships among local functional activity, energy metabolism, and blood flow in the central nervous system. Fed Proc 1981;40:2311–2316.
7. Lou HC, Edvinsson L, MacKenzie ET. The concept of coupling blood flow to brain function: revision required? Ann Neurol 1987;22:289–297.
8. Villringer A, Dirnagl U. Coupling of brain activity and cerebral blood flow: basis of functional neuroimaging. Cerebrovasc Brain Metab Rev 1995;7:240–276.
9. Jueptner M, Weiller C. Review: Does measurement of regional cerebral blood flow reflect synaptic activity?—Implications for PET and fMRI. Neuroimage 1995;2:148–156.
10. Lindauer U, Megow D, Schultze J, Weber JR, Dirnagl U. Nitric oxide synthase inhibition does not affect somatosensory evoked potentials in the rat. Neurosci Lett 1996;216:207–210.
11. Wolf T, Lindauer U, Villringer A, Dirnagl U. Excessive oxygen or glucose supply does not alter the blood flow response to somatosensory stimulation or spreading depression in rats. Brain Res 1997;761:290–299.
12. Fox PT, Raichle ME. Focal physiological uncoupling of cerebral blood flow and oxidative metabolism during somatosensory stimulation in human subjects. Proc Natl Acad Sci USA 1986;83:1140–1144.
13. Fox PT, Raichle ME, Mintun MA, Dence C. Nonoxidative glucose consumption during focal physiologic neural activity. Science 1988;241:462–464.
14. Ogawa S, Tank DW, Menon R, Ellermann JM, Kim SG, Merkle H, Ugurbil K. Intrinsic signal changes accompanying sensory stimulation: functional brain mapping with magnetic resonance imaging. Proc Natl Acad Sci USA 1992;89:5951–5955.
15. Buxton RB, Frank LR. A model for the coupling between cerebral blood flow and oxygen metabolism during neural stimulation. J Cereb Blood Flow Metab 1997;17:64–72.
16. Belliveau JW, Kennedy DN, Jr, McKinstry RC, Buchbinder BR, Weisskoff RM, Cohen MS, Vevea JM, Brady TJ, Rosen BR. Functional mapping of the human visual cortex by magnetic resonance imaging. Science 1991;254:716–719.
17. Frahm J, Merboldt KD, Hanicke W. Functional MRI of human brain activation at high spatial resolution. Magn Reson Med 1993;29:139–144.
18. Bock C, Schmitz B, Kerskens CM, Gyngell ML, Hossmann K-A, Hoehn-Berlage M. Functional MRI of somatosensory activation in rat: effect of hypercapnic upregulation on perfusion- and BOLD-imaging. Magn Reson Med 1998;39:457–461.
19. van Bruggen N, Busch E, Palmer JT, Williams S-P, Beaulieu C, de Crespigny A. High resolution functional MRI mapping of the rat cerebral cortex. J Cereb Blood Flow Metab 1997;17:S441.
20. Kerskens CM, Hoehn-Berlage M, Schmitz B, Busch E, Bock C, Gyngell ML, Hossmann K-A. Ultrafast perfusion-weighted MRI of functional brain activation in rats during forepaw stimulation: comparison with T2-weighted MRI. NMR Biomed 1996;9:20–23.
21. Kim SG. Quantification of relative blood flow change by flow-sensitive alternating inversion recovery (FAIR) technique: application to functional mapping. Magn Reson Med 1995;34:293–301.
22. Busch E, Hoehn-Berlage M, Eis M, Gyngell ML, Hossmann K-A. Simultaneous recording of EEG, DC potential and diffusion-weighted NMR imaging during potassium induced cortical spreading depression in rats. NMR Biomed 1995;8:59–64.
23. Frahm J, Haase A, Matthaei D. Rapid NMR imaging of dynamic processes using the FLASH technique. Magn Reson Med 1986;3:321–327.
24. Gyngell ML, Schmitz B, Hoehn-Berlage M, Hossmann K-A. Variation of functional MRI signal in response to frequency of somatosensory stimulation in alpha-chloralose anesthetized rats. Magn Reson Med 1996;36:13–15.
25. Paxinos G. The rat nervous system. San Diego: Academic Press; 1995.
26. McPherson RW, Zeger S, Traystman RJ. Relationship of somatosensory evoked potentials and cerebral oxygen consumption during hypoxic hypoxia in dogs. Stroke 1986;17:30–36.
27. Yamada S, Brauer F, Knierim D, Dayes L, Djernas M, Iacono R, Morgese V, Hayward W. Can somatosensory evoked potential monitoring predict energy dynamics during controlled hypotension? Neurol Res 1992;14:325–329.
28. Hyder F, Rothman DL, Mason GF, Rangarajan A, Behar KL, Shulman RG. Oxidative glucose metabolism in rat brain during single forepaw stimulation: a spatially localized $^{1}H(^{13}C)$ nuclear magnetic resonance study. J Cereb Blood Flow Metab 1997;17:1040–1047.
29. Leniger-Follert E, Hossmann K-A. Simultaneous measurements of microflow and evoked potentials in the somatomotor cortex of the cat brain during specific sensory activation. Pflugers Arch Eur J Physiol 1979;380:85–89.
30. Hossmann K-A, Schmitz B, Bock C, Kerskens C, Hoehn-Berlage M. Functional magnetic resonance imaging after cardiac arrest in rat. In: Krieglstein J, editor. Pharmacology of cerebral ischemia. Medpharm Scientific Publishers, Stuttgart 1996. p 357–365.
31. Ueki M, Linn F, Hossmann K-A. Functional activation of cerebral blood flow and metabolism before and after global ischemia of rat brain. J Cereb Blood Flow Metab 1988;8:486–494.
32. Schmitz B, Böttiger BW, Hossmann K-A. Functional activation of cerebral blood flow after cardiac arrest in rat. J Cereb Blood Flow Metab 1997;17:1202–1209.
33. Schmitz B, Bock C, Hoehn-Berlage M, Kerskens CM, Böttiger BW, Hossmann K-A. Recovery of the rodent brain after cardiac arrest: a functional magnetic resonance imaging study. Magn Reson Med 1998;39:783–788.
34. Bock C, Krep H, Brinker G, Hoehn-Berlage M. Brainmapping of alpha-chloralose anesthetized rats with T_2^*-weighted imaging: distinction between the representation of the forepaw and hindpaw in the somatosensory cortex. NMR Biomed 1998;11:115–119.